

# Induction of radioresistant nasopharyngeal carcinoma cell line CNE-2R by repeated high-dose X-ray irradiation

D. Zhu<sup>1</sup>, M. Huang<sup>1</sup>, M. Fang<sup>1</sup>, A. Li<sup>2</sup>, Z. Liu<sup>2</sup>, M. Shao<sup>1</sup>, Y. Liu<sup>1</sup>, J. Yang<sup>1</sup>,  
Q. Fan<sup>1\*</sup>

<sup>1</sup>School of Traditional Chinese Medicine, Southern Medical University, Guangdong Guangzhou, 510515, China

<sup>2</sup>NanFang Hospital, Guangdong Guangzhou, 510515, China

## ABSTRACT

**Background:** All To enhance the curative effect of radiotherapy, we established a radio-resistant cell line, CNE-2R from CNE-2, a radio-sensitive type of CNE, through repeated irradiation. The developed cell line provides a basis for further studies on the radio-resistance of CNE and the molecular mechanism of radiotherapy sensitization drugs. **Materials and Methods:** The CNE-2 cell line was selected and exposed repeatedly to high-dose X-ray intermittent irradiation (6 Gy/fraction for seven fractions and 20 Gy/fraction for three fractions). After the entire irradiation process, 20 Gy/time was administered to CNE irregularly. The cell growth curves of CNE-2 and CNE-2R were constructed based on MTT assays. Dose-survival curves were obtained through colony-forming tests and subjected to linear quadratic formulation matching. SF2 and correlation parameters of radiation biology were calculated. Changes in the cell cycle of CNE-2 and CNE-2R were also assessed by serum starvation. **Results:** The doubling time of CNE-2 was 2.4 days, which is 0.4 days shorter than that of CNE-2R, indicating the faster growth rate of CNE-2. In the dose-survival equation of the survival clone test, the sensitization ratio of CNE-2R was enhanced relative to that of CNE-2. After synchronization and desynchronization for 24 h, G1 was arrested in CNE-2R. In the S phase, which is insensitive to radiation, the ratio of G1 increased, hence altering the cell cycle. **Conclusion:** We have established a radio-resistant nasopharyngeal carcinoma cell line by repeated exposure to radiation which is relevant to changes in the cell cycle.

**Keywords:** Cell cycle, cell growth curve, cell radiation biology parameter, nasopharyngeal carcinoma, radio-resistance.

## ► Original article

### \*Corresponding authors:

Qin Fan, Ph.D.,

Fax: +86 20 6164 8244

E-mail:

fanqinshimen@yahoo.com

Revised: October 2018

Accepted: December 2018

Int. J. Radiat. Res., January 2019;  
17(1): 47-55

DOI: 10.18869/acadpub.ijrr.17.1.47

## INTRODUCTION

Nasopharyngeal carcinoma (NPC) is a malignant tumor prevalent in southern China <sup>(1)</sup>. Radiotherapy is the current primary treatment for NPC because of its anatomical characteristics <sup>(2,3)</sup>. Local residual or recurrence after radiotherapy commonly occurs because about 10%–20% of cells in NPC are resistant to radiation, thereby reducing the treatment effect <sup>(4-7)</sup>. In the present study, mainstream inducible methods were used to induce the NPC cell line CNE-2 to become a stable radio-resistant cell

subline for investigating the mechanism of radio-resistance <sup>(8-11)</sup>.

The mechanism underlying radiotherapy is DNA injury, particularly oxidative base damages, single-strand breaks, and double-strand breaks (DSBs) <sup>(12,13)</sup>; of these injury types, DSBs are confirmed to be the most lethal approach to DNA inactivation <sup>(14)</sup>. The lesions of DNA strands lead to chromosomal aberration, which increases genomic instability and inactivation of cancer cells. On the one hand, radio-sensitivity varies in different NPC cell lines (CNE) <sup>(12)</sup>. Radioactivity-induced lesions form the structure

of the human body, leading to radio-resistance and relapse as well as cancer spread and metastasis to normal tissues <sup>(15)</sup>.

Radiosensitivity weakens the curative effect of radiotherapy and is associated with the cell cycle and pathological grading. Proliferating cells exhibit stronger radio-sensitivity than non-proliferating cells; and chromosomal aberration during radiotherapy can occur in every phase of cell division <sup>(16)</sup>. Radioresistance is relevant to DNA repair capacity after radio-exposure because of the following reasons: 1. Radio-exposure may inactivate cells with high radio-sensitivity, thereby increasing the proportion of cells with high radio-resistance. 2. After radio-exposure, the DNA repair capacity increases, improving the radioresistance. 3. Chromosomal aberration during radio-exposure generates tumor cells with high radioresistance <sup>(17, 18)</sup>. Therefore, tumor cells with strong radioresistance can be obtained after repeated elimination and restoration under high-dose radiation culture for a long period.

To establish a radio-resistant nasopharyngeal carcinoma cell line that can be used as a model for the study of radiosensitization, our method innovatively combined the differences of the three common methods: 1. enhancing the largest dose to 20 Gy/time; 2. covering different phases of cell growth; 3. inducing radiosensitivity for a longer time, with certain radiation intervals at the earlier phase, and an uncertain radiation interval at the later phase; and 4. covering dose-rates in both certain and random condition.

We further probe the preliminary mechanisms of radiation resistance in the established nasopharyngeal carcinoma cell lines.

## **MATERIALS AND METHODS**

### ***Cell lines and culture***

Human CNE-2 (X-Ray-sensitive strains) cells were cultured in RPMI-1640 medium (GIBCO) supplemented with 10% fetal bovine serum (GIBCO), penicillin (50 mg/ml) (GIBCO), and

streptomycin (50 mg/ml) (GIBCO). The culture was maintained in 5% CO<sub>2</sub> in a humidified atmosphere at 37 °C. The spent growth medium was changed every day. The cells were detached with 0.25% trypsin and transferred after fusion growth.

### ***Irradiation***

In the first phase, CNE-2 cells were found to be in the logarithmic growth phase. The cells were washed twice with PBS solution, digested with 0.25% trypsin, and discarded after 3 min. The solution was added to a proper amount of RPMI-1640 containing 10% FBS medium and 1% penicillin-streptomycin solution and mixed homogeneously to prepare a single-cell suspension. The suspension was maintained in 5% CO<sub>2</sub>-humidified atmosphere at 37 °C for 24 h. The CNE-2 cells were subjected to X-ray irradiation using a medical linear accelerator. The radiation field was 25 cm × 25 cm, source-skin distance was 100 cm, the rate of radiation dose was 5.48 Gy/min, and the cover glass was 1 cm thick. The medium was changed immediately after irradiation, and the culture was transferred during fusion growth. The cells were irradiated again after attaining stable growth. The doses of X-ray radiation were 7 times of 6 Gy each and 3 times of 20 Gy each. In the second phase, the CNE-2 cells were immediately subjected to X-ray irradiation from a medical linear accelerator after transfer culture. The rate of radiation dose was randomly chosen, and the cells were irregularly irradiated with 20 Gy. In the third phase, the cells were alternately irradiated with one of the first two radiation methods chosen randomly. The entire process of irradiation and culture lasted for more than 12 months, and the total IR dose was largely more than 200 Gy.

### ***MTT assay***

An auxetic assay (MTT) was performed to investigate whether irradiated CNE-2 cell lines acquired radioresistance. The growth rates of CNE-2 and CNE-2R (radiation-induced CNE-2) cells were compared. Suspension cells were harvested by centrifugation. The cells were

released from their substrate by trypsinization and re-suspended at  $2 \times 10^3$ /ml. The cells were plated at  $2 \times 10^2$  per well into a 96-well cell culture cluster. Cell growth was examined by MTT assay for 8 consecutive days. After 0.5 mg/ml thiazolyl blue tetrazolium bromide (MTT, Sigma-Aldrich) was added to each well, the cells were incubated at 37 °C for 4 h. The formed crystals were solubilized in 100 µl of dimethyl sulfoxide (DMSO, Sigma-Aldrich) for 10 min at room temperature with strong agitation. Absorbance was read with a filter at 490 and 570 nm, and cell growth curve was constructed according to the daily mean of absorbance. The time for cell doubling was calculated by  $T_D = (t - t_0) \log_2 / \log N - \log N_0$ .

#### **Clonogenic survival assay**

Cells were counted and seeded at different cell densities in triplicates in six-well cell culture plates ( $1 \times 10^2$ ,  $1 \times 10^2$ ,  $1 \times 10^2$ ,  $2 \times 10^2$ ,  $2 \times 10^2$ ,  $2 \times 10^2$ ). After 24 h, the cells were irradiated with different doses of X-ray (0 Gy, 1 Gy, 2 Gy, 4 Gy, 6 Gy, and 8 Gy). After 7–14 days, the colonies were washed twice with PBS, fixed with ice-cold carbinol for 30 min, washed twice with PBS, stained with Giemsa solution (1:999 with distilled water) for 30 min, and washed with distilled water. Colonies with  $\geq 50$  cells were counted. Plating efficiency (PE) was calculated by dividing the number of colonies counted by the number of cells plated. The surviving fractions (SF) were calculated by dividing the PE by the PE of the non-irradiated control. Sensitization enhancement ratio was calculated by division of  $SF_2$ . Clonogenic survival curves were compared through the extra sum-of-squares F-test in GraphPad Prism.

#### **Assay using flow cytometry (FCM)**

Cells were cultured with serum-free 1640 medium for 36 h at a density of  $1.0 \times 10^6$  cells/ml and collected by centrifugation to investigate cell cycle synchronization with serum starvation. Portions of the cells were re-suspended in 200 µl of PBS. The remaining cells were cultured with 10% serum 1640 medium for 24 h. For cell cycle analysis, the cells were fixed with 75% ethanol at -20 °C overnight. On the following day, the

fixed cells were washed with PBS, treated with RNase A (50 µg/ml) in PBS at 37 °C for 30 min, and mixed with propidium iodide (PI, 50 µg/ml) for 30 min in the dark. The stained cells were analyzed with fluorescence-activated cell sorting (FACS) by FCM (FACS Calibur, Becton Dickinson, Bedford, MA).

#### **Twenty short tandem repeat assay**

Twenty short tandem repeat (STR) loci plus the gender determining locus, Amelogenin, were amplified using a commercially available STR profiling Kit. The cell line sample was processed using the ABI Prism® 3500XL Genetic Analyzer. Data were analyzed using GeneMapper® 5 software (Applied Biosystems).

Cell lines were authenticated using Short Tandem Repeat (STR) analysis as described in 2012 in ANSI Standard (ANSI/ATCC ASN-0002-2011 Authentication of Human Cell Lines: Standardization of STR Profiling) by the ATCC Standards Development Organization (SDO).

#### **Statistical analysis**

An independent two-sample *t*-test was used to assess the differences in continuous variables between the two independent groups. A *p*-value  $< 0.05$  indicates statistical significance. Statistical analyses were performed using SPSS 18.0 for Windows (SPSS, Chicago, IL, USA) and GraphPad Prism 6.0C for Mac (Prism, San Diego, California, USA).

## **RESULTS**

#### **Status of cell growth**

A cell growth curve is a basic index used to describe the biological characteristics of cells. This tool is important for observing the basic regularity of cell growth, which is also a significant index used in judging the vitality of cells. Cells derived from CNE-2 were named CNE-2R. The results of the MTT assay showed that CNE-2 cells entered the logarithmic growth phase in the third day after seeding, whereas CNE-2R cells entered the same phase on the fourth day. CNE-2 and CNE-2R cells entered a

plateau phase sixth and eighth day after seeding, respectively. The growth rate of CNE-2R was slower than that of the original cell line CNE-2.

According to the formula  $[TD = (t-t_0) \text{Log}2/\text{Log}N - \text{Log}N_0]$ , the doubling time of CNE-2 was 2.4 days and that of CNE-2R was 2.8 days (figure 1).

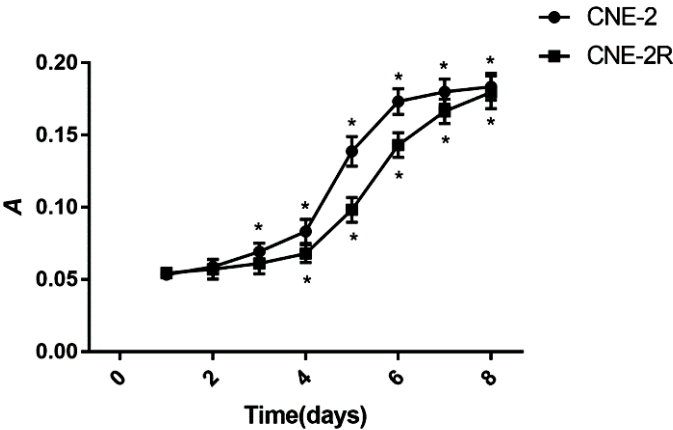


Figure 1. Cell growth curve of CNE-2 and CNE-2R cells.  
\*: Compared with First day,  $P < 0.05$

Changes in cell radiation biology parameter

A survival clone test can reveal the survival score of irradiated cells veritably and is thus widely used in measuring the radio-sensitivity of cells. In  $S = \exp (-\alpha D - \beta D^2)$ , which is the linear-quadratic formulation (L-Q) of cell-absorbed dose survival equation <sup>(19)</sup>,  $\alpha$  represents the cell lesion caused by low dose of radiation, and  $\beta$  represents the reduction factors dependent on irradiation time. The larger rate of  $\alpha/\beta$  indicates a weaker cell repair capacity, thereby directly reducing the radio-sensitivity of cells<sup>(20)</sup>. Under 2 Gy radiation, the higher survival fraction (SF2) indicates stronger radio- resistivity. We obtained CNE-2 and CNE-2R cells from three of the colony-forming test cells for L-Q matching and constructed the dose-survival curve (figure 2A). SF2 and the correlation parameters of radiation biology are shown in table 1. The  $\alpha/\beta$  of CNE-2 is  $23.4 \pm 4.16$ , whereas that of CNE-2R is  $6.71 \pm 1.13$  ( $P < 0.05$ ). The SF2 of CNE-2 is  $0.270 \pm 0.0275$ , whereas that of CNE-2R is  $0.663 \pm 0.0236$

( $P < 0.01$ ).

In a multi-target single-hit model, one of the most commonly used models in ionizing radiation sensitivity, N represents the cell repair capacity to radiation lesions- a larger N indicating a stronger cell resistance. The quasi-threshold dose (Dq) also has a direct ratio to cell resistance, whereas a larger mean lethal dose (D0) indicates stronger radio-resistance <sup>(21)</sup>. We took the CNE-2 and CNE-2R cells from three of the colony-forming test samples for multi-target single-hit model matching and obtained the dose-survival curve (figure 2B). The correlation parameters of radiation biology are shown in table 2. The D0 of CNE-2 is  $1.37 \pm 0.0985$ , and that of CNE-2R is  $2.99 \pm 0.475$  ( $P < 0.05$ ). The Dq of CNE-2 is  $1.52 \pm 0.115$ , and that of CNE-2R is  $3.45 \pm 0.417$  ( $P < 0.05$ ). The N of CNE-2 is  $1.16 \pm 0.034$ , and that of CNE-2R is  $1.58 \pm 0.104$  ( $P < 0.05$ ). As a result, the enhanced sensitization ratio in CNE-2R versus CNE-2 is  $0.469 \pm 0.0989$ .

Table 1. SF2 and the correlation parameters of radiation biology of CNE-2 and CNE-2R cells.

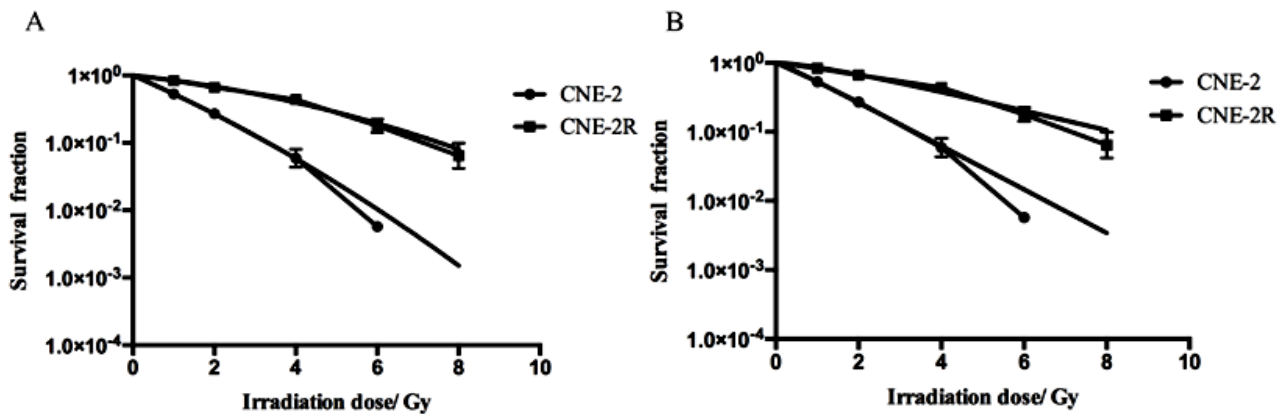
Cell line	$\alpha$ (Gy <sup>-1</sup> )	$\beta$ (Gy <sup>-2</sup> )	$\alpha/\beta$ (Gy)	SF <sub>2</sub>
CNE-2	0.609 ± 0.0566	0.0265 ± 0.00495	23.4 ± 4.16	0.270 ± 0.0275
CNE-2R	0.145 ± 0.0150	0.0222 ± 0.00576	6.71 ± 1.13	0.663 ± 0.0236
t	13.7	0.983	6.70	-18.8
p	0.00309*	0.382	0.0150*	0.000055*

\*:  $P < 0.05$

**Table 2.** Correlation parameters of multi-target single-hit model of CNE-2 and CNE-2R cells.

Cell line	D0	Dq	N	SER
CNE-2	1.37 ± 0.0985	1.52 ± 0.115	1.16 ± 0.034	—
CNE-2R	2.99 ± 0.475	3.45 ± 0.417	1.58 ± 0.104	0.469 ± 0.0989
t	-5, 79	-7.74	-6.79	—
P	0.0236*	0.0107*	0.0137*	—

\*: P &lt; 0.05

**Figure 2.** Dose-survival curve of CNE-2 and CNE-2R cells obtained from L-Q matching and multi-target single-hit model matching. A: L-Q matching; B: multi-target single-hit model matching

### Changes in the cell cycle

Serum starvation indicates that most of the cells are statically synchronized during the G0–G1 phase after cultivation in a serum-free medium for 24–48 h, whereas after de-synchronization by serum cultured for 24 h, the time and number of cells entering the next cycle are different, which can be detected by the retardant by FCM. We analyzed the proportion of the three phases of CNE-2 and CNE-2R cells (G0–G1, G2/M, and S phase) (figures 3-4). The proportions of cell cycle after 24 h of synchronization and desynchronization see in table 3. After synchronization and desynchronization for 24 h, less G1 ( $P < 0.05$ ) and more S ( $P < 0.05$ ) phase-cells of CNE-2R were observed compared with those of CNE-2. Among the CNE-2 cells, the ratio of cells at G1 reduced from 63.99% to 50.83% ( $P < 0.05$ ), whereas the ratio of cells at S rose from 35.35% to 47.54% ( $P < 0.05$ ). Among the CNE-2R cells, the ratio of

cells at G1 reduced from 45.92% to 43.86% ( $P > 0.05$ ), whereas the ratio of cells at S reduced from 54.02% to 52.46% ( $P > 0.05$ ), which indicated insignificant variation in the cells before and after the serum starvation test.

### STR profile report

The STR assay indicates that the radioresistant nasopharyngeal carcinoma cell line CNE-2R and the primary nasopharyngeal carcinoma cell line CNE-2 are derived from a common ancestry. Meanwhile, because the cells are passaged too many times, cell line CNE-2 has lost 5% STR message. Moreover, the radioresistant nasopharyngeal carcinoma cell line CNE-2R has lost 3% STR message more than CNE-2 because of irradiation (see in supplementary file). Only TH01 and vWA loci are different between CNE-2 and CNE-2R are shown in table 4.



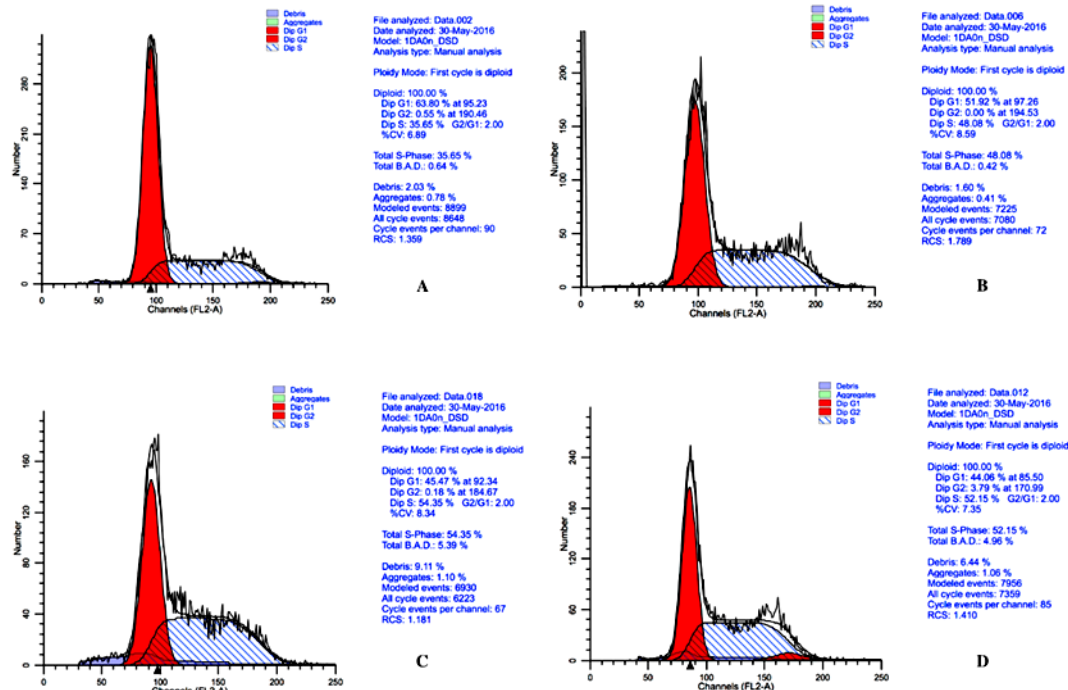


**Figure 3.** Changes in cell cycle after synchronization and desynchronization of CNE-2 and CNE-2R cells. **A:** Cell cycle of CNE-2 after synchronization. **B:** Cell cycle of CNE-2 after desynchronization for 24 h. **C:** Cell cycle of CNE-2R after synchronization. **D:** Cell cycle of CNE-2R after desynchronization for 24 h.

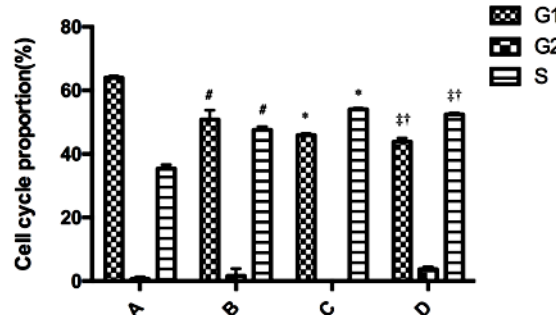


**Figure 4.** Changes in the proportions of cell cycle after 24 h of synchronization and desynchronization. **A:** Cell cycle of CNE-2 after synchronization. **B:** Cell cycle of CNE-2 after desynchronization for 24 h. **C:** Cell cycle of CNE-2R after synchronization. **D:** Cell cycle of CNE-2R after desynchronization for 24 h.

\*: C compare with A,  $P < 0.05$ ; †: D compare with B,  $P < 0.05$ ; #: B compare with A,  $P < 0.05$ ; ‡: D compare with C,  $P < 0.05$ .

**Table 3.** Changes in the proportions of cell cycle after 24 h of synchronization and desynchronization.

	G1	G2	S
A	63.9933±0.55582	0.6533±0.71066	35.3533±1.26144
B	50.8267±2.94629#	1.6333±2.26577	47.5400±1.12210#
C	45.9233±0.48809*	0.0600±0.10392	54.0167±0.40919*
D	43.8567±1.17823††	3.6833±0.82519	52.4633±0.43501††

A: Cell cycle of CNE-2 after synchronization.

B: Cell cycle of CNE-2 after desynchronization for 24 h.

C: Cell cycle of CNE-2R after synchronization.

D: Cell cycle of CNE-2R after desynchronization for 24 h.

\*: C compare with A,  $P < 0.05$ ; †: D compare with B,  $P < 0.05$ ; #: B compare with A,  $P < 0.05$ ; ‡: D compare with C,  $P < 0.05$

**Table 4.** The result of STR typing of CNE-2 and CNE-2R.

Samples Loci	CNE-2	CNE-2R
Amelogenin	X,X	X,X
D3S1358	15,18	15,18
D1S1656	12,15	12,15
D6S1043	11,14,18	11,14,18
D13S317	10,12,13.3	10,12,13.3
PentaE	17,20	17,20
D16S539	9,10	9,10
D18S51	13,16	13,16
D2S1338	17,23	17,23
CSF1PO	10,11	10,11
PentaD	9,12	9,12
TH01	6,7,9	6,9
vWA	14,17	14,16,17
D21S11	27,30	27,30
D7S820	10,12	10,12
D5S818	11,12	11,12
TPOX	8,9	8,8
D8S1179	12,13,17	12,13,17
D12S391	20,21	20,21
D19S433	13,13	13,13
FGA	18,21	18,21

## DISCUSSION

CNE is moderately sensitive to the majority of radioactive therapy, which makes it the treatment of choice for NPC worldwide.<sup>(15)</sup> However, research shows that loss in high sensitivity during radiotherapy can be attributed to radiation resistance of CNE. Moreover, radiotherapy can also cause genomic instability, which leads to recurrence and metastasis<sup>(12)</sup>. In this study, we used the CNE-2 cell line because of its high radio-sensitivity and low differentiation by pathology, which conforms to the characteristics of most types of CNEs and thus leads to a highly simulated clinical setting<sup>(22)</sup>. In addition, CNE-2R, the cell line with stable radioresistance, was obtained after more than 12 months of repeatedly high-dosed filtration and cultivation. By comparing the difference in radiation biological parameters of the two types of cells and the changes in cell cycle, the mechanism of radiation engendered on CNE cell proliferation, survival, and apoptosis could be revealed in a visual and

distinct way.

The cell cycle refers to the whole process from the start of one division to the end of the next, wherein the first division is split into the mitotic phase and interphase, whereas the latter is divided into G1/G0, S, and G2/M phase<sup>(23)</sup>. Radiation exposure has a retardant effect on all three phases, among which G1 checkpoint prevents damaged DNA from entering into the S phase to forward replication, and G2 checkpoint prevents the separation of abnormal chromosome in M phase<sup>(24)</sup>. As a result, the presence of arrest checkpoint extends the cell cycle. According to the result of FCM, we discovered that compared with CNE-2, the quantitative proportion of CNE-2R in G1 phase during the serum starvation test was not significantly lower after desynchronization and synchronization, indicating the existence of G1 phase arrest in CNE-2R and matching the 0.4-day extension of the doubling time of cell growth curve, which might be relevant to the activation of the checkpoint caused by radial lesion. Consistent with the report by Xiaohui Yu,

the radiation resistance of nasopharyngeal carcinoma cells is related to the G0/G1 cell cycle arrest caused by the high expression of CDC6 protein <sup>(25)</sup>.

Meanwhile, research had shown that radio-sensitivity to the same dose of irradiation of cells in different phases are diverse, showing that the G2/M phase has the highest radiosensitivity, whereas the S phase has the lowest. The results of FCM showed that, compared with CNE-2, the proportion of CNE-2R in G1 phase is significantly lower, whereas those in S phase is significantly higher <sup>(23)</sup>. Although the proportion of CNE-2R in G2 phase increased, it was still less than 4% of the quantum, indicating the increase in radio-resistance. The number of cells at the G0 phase was small due to dedifferentiation, hence their results were omitted in this study.

So far, there are three main methods to induce radio-resistant cell lines. The first one <sup>(26,27)</sup> is irradiating fewer times in larger-doses (5-10 Gy/time) on logarithmic-growth-phase-cells under a certain dose-rate, which induces cell lines with very unstable and weak radio-resistance. The second one <sup>(28-30)</sup> is irradiating several times in smaller-doses (1.5-3 Gy/time) before fewer times in larger-doses (6-10 Gy/time), which can induce cell lines with stable but weaker radio-resistance. Based on the latter, the third method<sup>17</sup> replaces logarithmic-growth-phase cells into slow phase cells. Our inducing method innovatively combined the differences of the three methods above: 1. Enhancing the largest dose into 20 Gy/time. 2. Covering different phases of cell growth. 3. Inducing for a longer time, with a certain radiation interval at the earlier phase while an uncertain radiation interval at the later phase. 4. Covering dose-rates in both certain and random condition. The objection of culturing for 12 months instead of few months is to assure the stability of resistance

The cell growth curve obtained from the MTT test suggested that the multiplication rate of CNE-2R was slower than that of CNE-2, indicating that the doubling time was longer and

verifying that CNE underwent cell cycle arrest after exposure to large-doses of radiation for a long period. Results obtained from L-Q of cell-absorbed dose survival equation showed that CNE-2R had a significantly higher survival fraction than CNE-2 when exposed to 2 Gy radiation, whereas the significantly lower  $\alpha/\beta$  in CNE-2R suggested a stronger repair capacity evolving to a stronger radio-resistance. Three or more Alleles at one or two loci may be due to somatic mutation, trisomy or gene duplications. Events with more than three alleles at more than three loci may be due to cellular contamination. In conclusion, the radio-stabilized CNE-2R cell induced by high-dose radiation can be the basis for future research on radio-resistance of CNE and the molecular mechanism of radiation-sensitive medicine. In the future, the apoptotic sensibility, genetic expression and primary culture of CNE-2R cells should be investigated.

## CONCLUSION

We have established a radio-resistant nasopharyngeal carcinoma cell line by repeated exposure to radiation which is relevant to changes in the cell cycle, and can be used as a model for studying radiosensitization of nasopharyngeal carcinomas.

## ACKNOWLEDGEMENT

*This work was supported by National Natural Science Foundation of China (grant No. 81673718, 81673628) and Guangdong Natural Science Foundation (grant No. 2016A030313833) and Science and Technology Project of Guangdong province (grant No. 2013A032500003, 2016A020226034) and Baiyun District of Guangzhou science and technology project (2016-KJ-001).*

**Conflicts of interest:** Declared none.



## REFERENCES

- Chia WK, Teo M, Wang WW, et al. (2014) Adoptive T-cell transfer and chemotherapy in the first-line treatment of metastatic and/or locally recurrent nasopharyngeal carcinoma. *Mol Ther*, **22(1)**: 132-139.
- Du C, Ying H, Zhou J, Hu C, Zhang Y (2013) Experience with combination of docetaxel, cisplatin plus 5-fluorouracil chemotherapy, and intensity-modulated radiotherapy for locoregionally advanced nasopharyngeal carcinoma. *Int J Clin Oncol*, **18(3)**: 464-471.
- Fahraeus R, Fu HL, Ernberg I, et al. (1988) Expression of Epstein-Barr virus-encoded proteins in nasopharyngeal carcinoma. *Int J Cancer*, **42(3)**: 329-338.
- Luftig M (2013) Heavy LIFTing: tumor promotion and radio-resistance in NPC. *J Clin Invest*, **123(12)**: 4999-5001.
- Lee AW, Ng WT, Chan LL, et al. (2014) Evolution of treatment for nasopharyngeal cancer—success and setback in the intensity-modulated radiotherapy era. *Radiother Oncol*, **110(3)**: 377-384.
- Suarez C, Rodrigo JP, Rinaldo A, Langendijk JA, Shaha AR, Ferlito A (2010) Current treatment options for recurrent nasopharyngeal cancer. *Eur Arch Otorhinolaryngol*, **267(12)**: 1811-1824.
- Yeh SA, Tang Y, Lui CC, Huang YJ, Huang EY (2005) Treatment outcomes and late complications of 849 patients with nasopharyngeal carcinoma treated with radiotherapy alone. *Int J Radiat Oncol Biol Phys*, **62(3)**: 672-679.
- Fang SU, Zhu XD, Song QU, Dan-Rong LI, Wei Z, Liang SX (2009) Establishment of a radioresistant subline from human nasopharyngeal carcinoma cell line and its cell cycle distribution pattern. *Chinese Journal of Cancer Prevention & Treatment*, **16(16)**: 1221-1224.
- Li G, Qiu Y, Su Z, et al. (2013) Genome-wide analyses of radioresistance-associated miRNA expression profile in nasopharyngeal carcinoma using next generation deep sequencing. *PLoS One*, **8(12)**: e84486.
- Chen ZT, Li L, Guo Y, et al. (2015) Analysis of the differential secretome of nasopharyngeal carcinoma cell lines CNE-2R and CNE-2. *Oncol Rep*, **34(5)**: 2477-2488.
- Guo S, Zhu X, Ge L, et al. (2015) RNAi-mediated knock-down of the c-jun gene sensitizes radioresistant human nasopharyngeal carcinoma cell line CNE-2R to radiation. *Oncology Reports*, **33(3)**: 1155-1160.
- Ward JF (1990) The yield of DNA double-strand breaks produced intracellularly by ionizing radiation: a review. *International Journal of Radiation Biology*, **57(57)**: 1141-1150.
- Wu TS, Lin BR, Chang HH (2015) Radio resistance mechanisms of cancers: An overview and future perspectives.
- Valerie K and Povirk LF (2003) Regulation and mechanisms of mammalian double-strand break repair. *Oncogene*, **22(37)**: 5792-5812.
- Mladenov E, Magin S, Soni A, Iliakis G (2013) DNA double-strand break repair as determinant of cellular radiosensitivity to killing and target in radiation therapy. *Frontiers in Oncology*, **3**: 113.
- Kastan MB and Bartek J (2004) Cell-cycle checkpoints and cancer. *Nature*, **432(7015)**: 316-323.
- Cheng JJ, Hu Z, Xia YF, Chen ZP (2006) [Radioresistant subline of human glioma cell line MGR2R induced by repeated high dose X-ray irradiation]. *Ai Zheng*, **25(1)**: 45-50.
- Nicolay NH, Perez RL, Saffrich R, Huber PE (2015) Radio-resistant mesenchymal stem cells: mechanisms of resistance and potential implications for the clinic. *Oncotarget*, **6(23)**: 19366-19380.
- Rossi HH and Kellere AM (1972) Radiation carcinogenesis at low doses. *Science*, **175(4018)**: 200-202.
- Rossi HH, Hall EJ, Kellere AM (1973) Biophysical factors in brachytherapy with low- and high-LET radiations. *Radiology*, **107(3)**: 645-649.
- Xinchen, Ruizhi, Yuxia, et al. (2007) Effects of Tetrandrine on Apoptosis and Radiosensitivity of Nasopharyngeal Carcinoma Cell Line CNE. *Acta Biochimica Et Biophysica Sinica*, **39(11)**: 869-878.
- Wang S, Guo CY, Castillo A, Dent P, Grant S (1998) Effect of bryostatin 1 on taxol-induced apoptosis and cytotoxicity in human leukemia cells (U937). *Biochemical Pharmacology*, **56(5)**: 635-644.
- Sinclair WK and Morton RA (1966) X-ray sensitivity during the cell generation cycle of cultured Chinese hamster cells. *Radiation Research*, **29(3)**: AV88-101.
- Kaufmann WK and Paules RS (1996) DNA damage and cell cycle checkpoints. *Faseb Journal Official Publication of the Federation of American Societies for Experimental Biology*, **10(2)**: 238-247.
- Yu X, Liu Y, Yin L, et al. (2018) Radiation-promoted CDC6 protein stability contributes to radioresistance by regulating senescence and epithelial to mesenchymal transition. *Oncogene*, 2018.
- Sun L, Moritake T, Zheng Y, et al. (2013) *In vitro* stemness characterization of radio-resistant clones isolated from a medulloblastoma cell line ONS-76. *Journal of Radiation Research*, **54(1)**: 61-69.
- Xie L, Song X, Yu J, et al. (2009) Fractionated irradiation induced radio-resistant esophageal cancer EC109 cells seem to be more sensitive to chemotherapeutic drugs. *Journal of Experimental & Clinical Cancer Research*, **28(1)**: 68.
- Li Z, Yang X, Xia N, et al. (2014) PTOP and TRF1 help enhance the radio resistance in breast cancer cell. *Cancer Cell International*, **14(1)**: 7.
- Ye F, Zhang Y, Liu Y, et al. (2013) Protective properties of radio-chemoresistant glioblastoma stem cell clones are associated with metabolic adaptation to reduced glucose dependence. *PLOS ONE*, **8(11)**.
- Falcão PL, Motta BM, De Lima FC, Lima CV, De Campos TPR (2015) Enhancement of viability of radiosensitive (PBMc) and resistant (MDA-MB-231) clones in low-dose-rate cobalt-60 radiation therapy. *Radiologia Brasileira*, **48(3)**: 158-165.

